TD-BEM for Sound Radiation in three Dimensions and the Numerical Evaluation of Retarded Potentials

M. Maischak[1], E. Ostermann[2], E. P. Stephan[3]

[1] *Brunel University, United Kingdom, Email: matthias.maischak@brunel.ac.uk*

[2] *Leibniz University Hannover, Germany, Email: osterman@ifam.uni-hannover.de*

[3] *Leibniz University Hannover, Germany, Email: stephan@ifam.uni-hannover.de*

Introduction

Due to the progress in computational power and a better understanding of the mathematical theory, the time domain boundary element method (TD-BEM) is recently gaining influence in the modeling of radiation phenomena. Parallel programming gave rise to computations of real life problems in a reasonable time.

In this paper we choose a simple model problem, namely the retarded single layer ansatz, to explain the underlying space-time Galerkin method as proposed by Ha-Duong, cf. [3, 4] and the references therein. We pay special attention to the evaluation of the matrix entries involved and briefly explain the storage scheme. Moreover, we present some numerical experiments also exploring the performance of the parallel computation of the matrices involved and discuss the realization of a marching-on-in-time (MOT) algorithm.

Model Problem

Consider the transient sound radiation of some simply connected bounded domain Ω^- into its open complement $\Omega := \mathbb{R}^3 \setminus \overline{\Omega^-}$. We investigate the wave equation for the displacement $u(t,x)$ with $t \in \mathbb{R}_+$, $x \in \Omega$

$$\frac{\partial^2 u}{\partial t^2} - \Delta u = 0. \tag{1}$$

Assume causal functions vanishing for $t < 0$. u satisfies the initial conditions

$$u(0,x) = \frac{\partial u}{\partial t}(0,x) = 0 \quad \text{for } x \in \Omega \tag{2}$$

and Dirichlet boundary conditions on $\Gamma := \partial\Omega$

$$u = f \quad \text{on } \mathbb{R} \times \Gamma. \tag{3}$$

Use a single layer potential ansatz for the solution u, such that for $x \notin \Gamma$

$$u(t,x) = Sp(t,x) = \frac{1}{4\pi} \int_\Gamma \frac{p(t-|x-y|,y)}{|x-y|} ds_y$$

with density function p and the retarded time argument $\tau := t - |x-y|$. The latter connects the space and time variables and physically results in the retarded signal of a source point. As we will see later, this retarded time argument has a significant impact on our discretization scheme. As the single layer potential S is continuous, we have for its limit on Γ with $x \in \Gamma$

$$Vp(t,x) = \frac{1}{4\pi} \int_\Gamma \frac{p(t-|x-y|,y)}{|x-y|} ds_y \tag{4}$$

and using (3), there holds the boundary integral equation for p

$$f(t,x) = Vp(t,x). \tag{5}$$

In [4] the following space-time variational formulation is proposed. Find $p(t,x)$ for $x \in \Gamma$, $t \in [0,T]$

$$\int_0^\infty \int_\Gamma Vp(t,x)\dot\eta(t,x) ds_x\, dt = \int_0^\infty \int_\Gamma f(t,x)\dot\eta(t,x) ds_x\, dt \tag{6}$$

for appropriate test functions $\dot\eta(t,x)$. Here the dot indicates the time derivative. Due to the theory of Ha-Duong [4] this formulation is uniquely solvable in appropriate Sobolev spaces on Γ and $[0,\infty)$. It can be solved approximately using finite element subspaces in space and time. For some convergence results see [4] and the references therein.

Space-Time Discretization

Choose a triangulation $\mathcal{T}_h$ of Γ into triangles and let $V_h \subset H^{-1/2}(\Gamma)$ denoted by $V_h = S_h^{p_s}$, where p_s indicates the polynomial degree of the functions and h is the maximal diameter of all triangles in $\mathcal{T}_h$. Then the density p can be approximated in space by

$$p_h(t,x) = \sum_{i=1}^{N_s} \alpha_i(t)\varphi_i(x) \quad \text{where } \varphi_i \in V_h.$$

Decompose the time interval $(0,\infty)$ into uniform subintervals $\mathcal{I}_m := (t_{m-1}, t_m]$ of size Δt and with $t_m = m\Delta t$ for $m = 0, \ldots$. We represent $\alpha_i(t) = \sum_{m=1}^{N_t} \phi_i^m \gamma^m(t)$ with basis functions γ^m for $m = 1, \ldots, N_t$ on a finite time intervall $[0,T]$. Thus for test functions $\eta(t,x) = \gamma^n(t)\varphi_j(x)$ the discrete approximation of (6) reads

$$\sum_{m=1}^{N_t} \sum_{i=1}^{N_s} \phi_i^m \int_\Gamma \int_\Gamma I^{n-m}(x,y) \frac{\varphi_i(y)\varphi_j(x)}{|x-y|} ds_y\, ds_x, \tag{7}$$

where we evaluate the integral

$$I^{n-m}(x,y) := \int_0^\infty \gamma^m(t-|x-y|)\dot\gamma^n(t)\, dt \tag{8}$$

analytically. For constant basis functions in time

$$\gamma^n(t) = \begin{cases} 1 & t \in \mathcal{I}_n \\ 0 & \text{else} \end{cases}$$

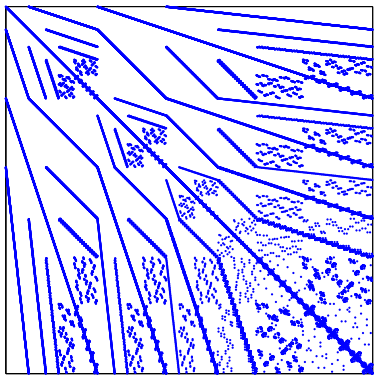

Figure 1: Sparsity pattern of retarded matrix V^0 on sphere surface with 5120 elements. 0.25% non-vanishing entries.

we obtain for (8)

$$I^{n-m}(x,y) = \begin{cases} 1 & (x,y) \in E_{n-m-1} \\ -1 & (x,y) \in E_{n-m} \\ 0 & \text{else} \end{cases}$$

where

$$E_k := \{(x,y) \in \Gamma \times \Gamma \,:\, t_k \le |x-y| \le t_{k+1}\}\,.$$

We refer to E_k as light cone integration domain or domain of influence. One observes, that the value of I^{n-m} depends only on the time difference. This gives rise to a time stepping procedure, namely

$$V^0 \phi^n = F^n - \sum_{m=1}^{n-1} V^{n-m} \phi^m$$

for $n = 1, \ldots, N_t$, where for piecewise constant basis functions in time we have

$$V_{ij}^k = \iint\limits_{E_{k-1}} \frac{\varphi_i(y)\varphi_j(x)}{|x-y|}\, ds_y\, ds_x - \iint\limits_{E_k} \frac{\varphi_i(y)\varphi_j(x)}{|x-y|}\, ds_y\, ds_x$$

$$\phi^m = (\phi_1^m, \ldots, \phi_{N_t}^m)^T$$

$$F_j^n = \int_\Gamma \left(f(t_{n-1},x) - f(t_n,x)\right) \varphi_j(x)\, ds_x.$$

In each time step, we have to compute a new matrix V^{n-1} and a new solution vector ϕ^n. The matrices V^k are sparsely populated, compare Figure 1, as we have a light cone integration domain E_k, such that only elements whose distance is in a certain range interact. Another remarkable fact is, that we have the same system matrix V^0 in each time step.

Computation of Matrix Entries

The computation of a matrix entry V_{ij}^k always involves the computation of an integral

$$G_{ij}^k = \iint\limits_{E_k} \frac{\varphi_i(y)\varphi_j(x)}{|x-y|}\, ds_y\, ds_x.$$

First of all, it is sensible to compute this basic integral only once and to reuse it in the next time step, as

$$V_{ij}^{k+1} = G_{ij}^k - G_{ij}^{k+1}.$$

In the following, we discuss the efficient computation of G_{ij}^k and the underlying MOT-algorithm. For this purpose fix the time dependent radii to $r_{\max} = t_{k+1}$ and $r_{\min} := t_k$ and regard the prototype integral

$$G_{ij} := \iint\limits_E k_\nu(|x-y|)\varphi_i(y)\varphi_j(x)\, ds_y\, ds_x \qquad (9)$$

with $k_\nu(z) = z^\nu$ and

$$E := \{(x,y) \in \Gamma \times \Gamma \text{ s.t. } r_{\min} \le |x-y| \le r_{\max}\}\,.$$

Moreover, define the point light cone or the domain of influence of point $x \in \mathbb{R}^3$ by

$$E(x) := \left\{y \in \mathbb{R}^3 \text{ s.t. } r_{\min} \le |x-y| \le r_{\max}\right\}.$$

and the domain of influence of a triangle T by

$$E(T) := \{y \in \mathbb{R}^3 : r_{\min} \le |x-y| \le r_{\max}\,,\, x \in T\}.$$

In Figure 4 the domain of influence $E(T_{i'})$ intersected with the triangle plane is sketched. Before we discuss the numerical evaluation of (9), let us discuss an simplified test for the potential interaction of two elements in E, because if two elements do not interact, the corresponding integral vanishes and we can use the below described test for the storage allocation in our matrices. The domain of interaction of two elements T_i and T_j in the light cone E satisfies

$$E \cap (T_i \times T_j) \subset (T_i \cap E(T_j)) \times (E(T_i) \cap T_j).$$

Let $B_{r_k}(m_k)$ denote the circumsphere of triangle T_k with center m_k and radius r_k $(k = i, j)$. The domain of influence $E(T_k)$ is a subset of an annular domain defined by its circumsphere

$$E(T_k) \subset C(T_k) := B_{r_k + r_{\max}}(m_k) \setminus B_{(r_{\min} - r_k)_+}(m_k).$$

Thus, a simple test on the element interaction of two elements in a light cone E is

$$E \cap (T_i \times T_j) \subset (T_i \cap C(T_j)) \times (C(T_i) \cap T_j). \qquad (10)$$

One can rewrite (9) as

$$G_{ij} = \sum_{\substack{T_{i'} \subset \text{ supp } \varphi_i \\ T_{j'} \subset \text{ supp } \varphi_j}} \iint\limits_{E \cap (T_{i'} \times T_{j'})} k_\nu(|x-y|)\varphi_i(y)\varphi_j(x)\, ds_y\, ds_x$$

$$= \sum_{\substack{T_{i'} \subset \text{ supp } \varphi_i \\ T_{j'} \subset \text{ supp } \varphi_j}} \int\limits_{T_{j'} \cap E(T_{i'})} \varphi_j(x) P_{i,i'}(x)\, ds_x \qquad (11)$$

where we define the retarded potential $P_{i,i'}$ via

$$P_{i,i'}(x) := \int\limits_{E(x) \cap T_{i'}} k_\nu(|x-y|)\varphi_i(y)\, ds_y. \qquad (12)$$

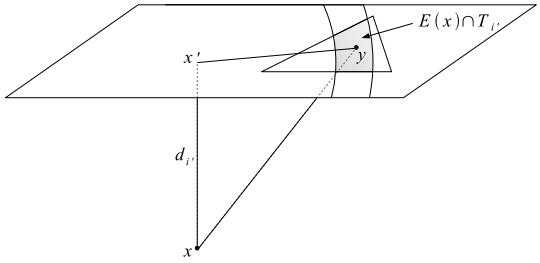

Figure 2: Projection of x onto the triangle plane.

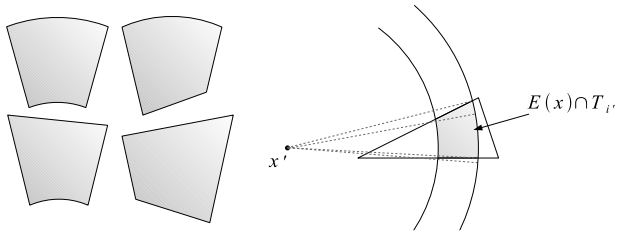

Figure 3: Example for a decomposition of $E(x) \cap T_{i'}$ with respect to x' and the four generic subdomains.

Composite Quadrature rule for $P_{i,i'}$

First of all, we have to find a parametric representation of the integration domain $E(x) \cap T_{i'}$. The domain of influence of point x is an annular domain with center x and radii $r_{\min}$ and $r_{\max}$. Therefore, we have to find the intersection of triangle $T_{i'}$ with two spheres. This three dimensional intersection problem can be reduced to a two dimensional intersection in a three dimensional space. Let x' denote the orthogonal projection of x onto the triangle plane and (cf. Figure 2) and define $d_{i'} := |x - x'|$. Then $E(x)$ intersected with the triangle plane is

$$E_{i'}(x) := \left\{ y \in \mathbb{R}^3 \ : \ \tilde{r}_{\min} \leq |x - y| \leq \tilde{r}_{\max} \right\},$$

where $\tilde{r}_{\min\,/\,\max} := (r^2_{\min\,/\,\max} - d^2_{i'})^{1/2}$ and thus

$$E(x) \cap T_{i'} = E_{i'}(x') \cap T_{i'}.$$

Introduce polar coordinates (r, θ) with respect to x' and decompose $E_{i'}(x') \cap T_{i'} = \bigcup_{l=1}^{n_d} D_l$ into $n_d \leq 15$ subdomains defined by

$$D_l := \left\{ (r, \theta) \ : \ \theta \in \mathcal{I}_{\theta_l} \text{ and } r \in (r_1^l(\theta), r_2^l(\theta)) \right\},$$

where $\mathcal{I}_{\theta_l} := (\theta_l, \theta_{l+1})$. $r^l_{1,2} = r_{\min\,/\,\max}$, if the upper or lower boundary with respect to r is one of the intersecting circles. If it is a triangle edge e with outer normal n and vertex v, it holds

$$r_e(\varphi) = \frac{v \cdot n}{n_1 \cos\varphi + n_2 \sin\varphi}.$$

In Figure 3 an example for such an decomposition is given and the four generic subdomains are sketched. Now, we

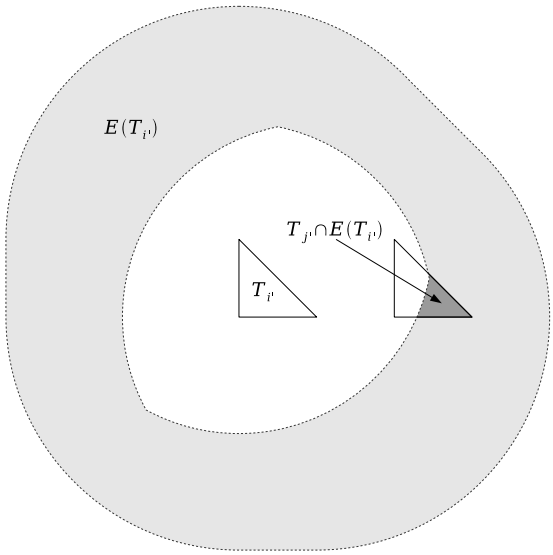

Figure 4: Intersection of triangle $T_{j'}$ with the domain of influence of element $T_{i'}$.

can rewrite (12), such that

$$\begin{aligned} P_{i,i''}(x) &= \sum_{l=1}^{n_d} \int_{D_l} (d_{l'}^2 + r^2)^{\frac{\nu}{2}} \varphi_i(r, \theta) r(\varphi) \, dr \, d\theta \\ &\approx \sum_{l=1}^{n_d} \mathcal{Q}_{l,k} \left[(d_{i'}^2 + r^2)^{\frac{\nu}{2}} \varphi_i(r, \varphi) r(\varphi) \right]. \end{aligned}$$

The quadrature rule $\mathcal{Q}_{l,k}$ denotes a the tensor product of the k-point Gaussian quadrature rule in θ and the k-point Gaussian quadrature in r-direction skaled to D_l. Moreover, we apply an additional grading depending on the kernel function k_ν and the regularity of r_l, details may be found in [6].

Composite Quadrature rule for G_{ij}

If we now return to (11), a quadrature rule for the remaining outer integral with respect to x has to be found. Here, the integration domain $T_{j'} \cap E(T_{i'})$ is the intersection of the domain of influence of $T_{i'}$ and the element $T_{j'}$. A sketch of such an intersection can be found in Figure 4. One may ask, why such an complicated looking decomposition is necessary, but as we seek to use Gaussian quadrature, we have to make sure, that the integrated function $P_{i,i'}$ is sufficiently smooth. The support of $P_{i,i'}$ is $E(T_{i'})$ and additionally to this cut-off behavior, we observed singularities in the second derivatives of $P_{i,i'}$, which will be especially troublesome for higher order test functions in space. For details we again refer to [6] and [1].

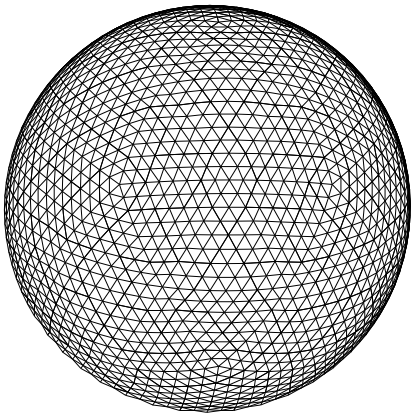

Figure 5: Mesh of the surface of the sphere with 5120 elements.

$i = 1$;
for $n = 1, \dots N_t$ **do**
  if $G^{n-2} = 0$ *or* $i > 1$ **then**
    Domain of influence has passed the body
    No more matrix evaluation needed;
    $i = i + 1$
  else
    Allocate storage for G^{n-1} using (10);
    Compute G^{n-1};
    $V^{n-1} = G^{n-2} - G^{n-1}$;
    Delete G^{n-2};
  end
  Compute right hand side
  $R^n = F^n - \sum_{m=i}^{n-1} V^{n-m}\phi^m$;
  Solve $V^0\phi^n = R^n$;
  Store new solution vector ϕ^n.
end

Algorithm 1: Time Stepping Algorithm

Numerical Examples

The numerical example uses a benchmark provided in [5]. We apply the above described retarded single layer ansatz with a space time Galerkin discretization. The surface mesh of $\Gamma := \partial B_1(0)$ is generated by a recursive refinement of the icosahedron, compare Figure 5. All computation were done in the program package MaiProgs [2]. The matrix computation, the most expensive part, is parallelized using OpenMP. The results presented are computed on a Dual-Intel Xeon 2,5 GHz with 8 cores and 8GB. The time step size was $\Delta t = 0.03125$ and for 5120 elements the ratio between time and space step size was 0.378. For this configuration the first 64 matrices have to be stored, because for larger time steps the domain of E has passed Γ and the integration domain vanishes. The matrix entries were computed using the composite quadrature rule for P as explained before and a standard hp-quadrature for the outer integral (11) with a grading strategy toward the vertices and edges of the element in the near field and a standard quadrature in the far field. A decomposition in the according element light cone is currently work in progress. In Figure 6(a) the percentage of allocated matrix entries is compared with the percentage of actually non-vanishing matrix entries.

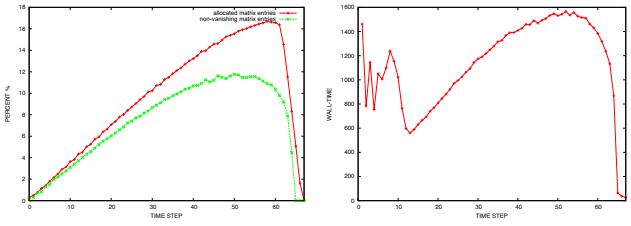

(a) Allocated matrix entries (red) and actually non vanishing matrix entries (green).

(b) Wall time (sec) per matrix.

Figure 6: Comparison of storage allocation and computation times.

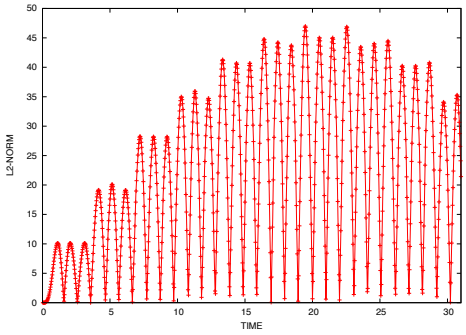

Figure 7: Long time stability ($t = 0 \dots 31$).

In Figure 6(b) the wall time for the matrix computation is plotted for each time step. The first matrix V^0 (cf. Figure 1) was computed with greater accuracy, as it is the system matrix. Due to the grading quadrature in the near field the first few matrices are quite expensive, although they are relatively sparse compared to later time steps. Although the outer quadrature is not yet optimal, we obain a longtime stable solution as plotted in Figure 7 for 1000 time steps.

References

[1] E. P. Stephan, M. Maischak, E. Ostermann. Transient Boundary Element Method and Numerical Evaluation of Retarded Potentials. Computational Science – ICCS 2008 **5102** (2008), 321-330

[2] Reference to the MaiProgs homepage. URL: `http://www.ifam.uni-hannover.de/~maiprogs`

[3] T. Ha-Duong, B. Ludwig, I. Terrasse. A Galerkin BEM for transient acoustic scattering by an absorbing obstacle. Internat. J. Numer. Methods Engrg. **57** (2003), 1845-1882

[4] T. Ha-Duong. On retarded potential boundary integral equations and their discretisation. Lect. Notes Comput. Sci. Eng. **31** (2003), 301–336

[5] L. Banjai, S. Sauter. Rapid solution of the wave equation in unbounded domains. SIAM J. Numer. Anal. **47** (2008/2009), 227-249

[6] E. Ostermann. Efficient quadrature methods for retarded boundary integral equations. PhD thesis. (in preparation)